sustainability

MDPI

Article

The Estimation of Forest Carbon Sink Potential and Influencing Factors in Huangshan National Forest Park in China

Wenduo Huang [1], Xiangrong Wang [1,*] and Dou Zhang [2,*]

[1] Department of Environmental Science and Engineering, Fudan University, Shanghai 200433, China; huangwenduo1003@gmail.com
[2] School of Civil Engineering and Architecture, Zhejiang Sci-Tech University, Hangzhou 310018, China
* Correspondence: xrxrwang@fudan.edu.cn (X.W.); zhangdou@zstu.edu.cn (D.Z.); Tel.: +86-13601682126 (X.W.)

Abstract: In this study, the biomass expansion factor (BEF) method was combined with the tree growth function in order to obtain a more accurate growth function of tree species through the fitting of different growth functions to tree growth, and to determine the characteristics of the forest carbon stock as well as the carbon sink potential of Huangshan National Forest Park (HNFP) in China. The carbon sink potential of each tree species and the integrated influencing factors, such as the stand and soil, were directly represented by structural equation modelling (SEM) to clarify the size and path of each influencing factor against the carbon sink potential. The results showed the following: (1) the logistic growth function fitting results for the seven major tree species in HNFP were better than those from the Richard–Chapman growth function, and the R^2 was greater than 0.90. (2) In 2014, the total carbon stock of the forest in HNFP was approximately 9.59×10^5 t, and the pattern of carbon density, in general, was higher in the central region and the northeastern region and lower in the northern and southern regions, while the distribution of carbon density was lower in the northern and southern regions. The carbon density pattern generally showed a higher distribution in the central and northeastern regions and a lower distribution in the northern and southern regions; most of the high-carbon-density areas were distributed in blocks, while the low-carbon-density areas were distributed sporadically. (3) The total carbon sink of the forest in HNFP was 8.26×10^3 t in 2014–2015, and due to the large age structure of the regional tree species, the carbon sinks of each tree species and the total carbon sink of HNFP showed a projected downward trend from 2014 to 2060. (4) For different tree species, the influencing factors on carbon sink potential are not the same, and the main influence factors involve slope position, slope, altitude, soil thickness, etc. This study identified the carbon stock and carbon sink values of the forest in HNFP, and the factors affecting the carbon sink potential obtained by SEM can provide a basis for the selection of new afforestation sites in the region as well as new ideas and methods to achieve peak carbon and carbon neutrality both regionally and nationally in the future.

Keywords: BEF; tree growth function; SEM; carbon stock; carbon sink potential; HNFP; China

Citation: Huang, W.; Wang, X.; Zhang, D. The Estimation of Forest Carbon Sink Potential and Influencing Factors in Huangshan National Forest Park in China. *Sustainability* **2024**, *16*, 1351. https://doi.org/10.3390/su16031351

Academic Editors: Alessandra De Marco and Roberto Mancinelli

Received: 15 November 2023
Revised: 28 January 2024
Accepted: 1 February 2024
Published: 5 February 2024

1. Introduction

The excessive extraction and utilization of energy by humans have led to an overabundance of carbon from fossil fuels being released into the atmosphere [1], posing a considerable challenge that urgently needs to be addressed: the continual rise in global temperatures due to these greenhouse gases [2]. The Paris Agreement [3] aims to keep the global average temperature increase well below two degrees Celsius above pre-industrial levels, and as a signatory, China has set strategic targets to ensure peak carbon emissions by 2030 and achieve carbon neutrality by 2060.

Terrestrial vegetation has been an invisible yet significant force against global warming [4,5] that has played a substantial role over the past three decades [6], with forests, in particular, serving as an irreplaceable factor in reducing the accumulation of greenhouse

gases in the atmosphere [7]. China has long been committed to forest conservation, implementing afforestation, reforestation, and the establishment of protected areas. These initiatives have significantly increased both the area of forested land [8] and the forest carbon sink capacity [9] in the past thirty years, mitigating China's greenhouse effect to a certain extent [10]. China's afforestation efforts have contributed to a notable carbon sink [11]; however, studies indicate that the carbon sink potential of existing forests is set to inevitably decline in this century [12]. Therefore, scientifically planning the timeline for tree planting and forest carbon sinks based on the overall future potential is critically important [13,14]. Investigating the impacts of environmental factors on the forest carbon sink potential can aid in formulating more efficient forest management decisions [15–17], thereby enhancing the long-term carbon sink capability of forests [16,18,19] and strengthening their role in mitigating global warming. Huangshan National Forest Park (HNFP) serves as a successful case of forest conservation in China, where, under governmental management, it has been well protected with minimal human interference, offering an excellent opportunity to study the impact of geographic factors on a forest carbon sink. Furthermore, diverging from the traditional approach of evaluating the carbon sink potential based on forest types [20,21], research at the species scale aligns more closely with the characteristics of afforestation in smaller areas (which involve specific tree species). This research methodology and its findings are better suited to the precise management of regional afforestation efforts.

Existing methods for estimating carbon sinks in forest ecosystems include the forest ecosystem carbon stock estimation method [22], the forest carbon balance modelling method [23], and the forest ecosystem carbon flow estimation method [24]. Among them, the forest ecosystem carbon stock estimation method, which calculates the carbon stock and then obtains the potential of the carbon sinks, has been widely used due to its low operational difficulty, high reliability, and wide range of applications. Among forest carbon stock estimation methods, the direct measurement method [25] requires high forest data, the remote sensing method [26] tends to estimate forest carbon stock at a large scale, and the biomass expansion factor (BEF) method is more practical and accurate in the absence of detailed information on tree measurement factors. The BEF method was proposed by Fang et al. and has played a transformative role in accurately estimating carbon stocks in China [21]; it has been applied in Europe [27], and the Americas [28]. The forest carbon sink potential can be converted to the difference between the year of maximum forest carbon stock and the forest carbon stock of a certain year, and because the growth of trees has a maximum limit, the carbon stock of mature forests (or overmature forests) can be regarded as the maximum carbon stock in the region [29]; thus, we can derive the total carbon sink potential of regional forests.

Considering the growth process of trees, the increase in the forest carbon stock in forest ecosystems is mainly caused by the increase in tree carbon density with the increase in age; ecologists believe that the changes in tree carbon density and age are closely related [30], and it is generally believed that the change in tree carbon density with age is consistent with the logistic, Richard–Chapman, and Gompertz growth functions, among others [31]. Studies have used tree age to calculate the carbon density of trees to obtain the carbon sink potential of forests in both large areas [9,21] and small areas [20,32]. Due to differences in the growth rates and conditions of different tree species, to obtain more accurate carbon stocks in forest ecosystems, different growth functions for different tree species can improve the accuracy of forest ecosystem carbon stocks, and thus improve the accuracy of carbon sink calculations.

Forest carbon stock is an important indicator for studying the exchange of carbon between forest ecosystems and the atmosphere. Existing studies have explored many factors affecting forest carbon stock, including environmental factors [33,34], climatic factors [35], and artificial influences [36]. However, carbon stocks vary depending on the population composition and dominant species type [37], and a selection of carbon stock studies ignore the growth condition of forests and so cannot directly reflect the response of

forest ecosystems. Carbon sink potential refers to the amount of carbon that can be absorbed and stored by forest ecosystems within a certain period in the future, and it is an important indicator for assessing the responsiveness of forest ecosystems to climate change. Therefore, studying the influencing factors of carbon sink potential can help us to understand the responsiveness of forest ecosystems and develop corresponding management strategies. In the past, most studies have focused on single aspects such as the altitude factor, landform, canopy density, etc. [35,38], with fewer indirect studies focusing on the interactions between influencing factors and these features. In fact, in addition to the factors directly affecting carbon sink potential, some environmental factors may affect carbon sink potential through indirect pathways. Such studies can be more comprehensive and integrated to analyze the effects of various factors such as site conditions and stand density.

In terms of study methodologies, SEM has become one of the main methods for contemporary ecological data analysis [39]. Unlike other multivariate statistical methods, SEM is driven by theoretical assumptions and can not only obtain correlations among variables, but can quantify direct and indirect causal relationships among multiple variables simultaneously [40,41]. The application of SEM to the study of factors influencing the potential of carbon sinks can directly determine the directions and magnitudes of the influences of environmental factors on the potential of carbon sinks, which provides new perspectives.

HNFP is an important natural ecological reserve, forest park, and geological park, and the forest diversity in the park is of national and global conservation significance [42]. In this study, we chose HNFP in Anhui Province, China, as a case study, and the objectives of the study were (1) to simulate relationships between the carbon stocks of different tree species and forest ages in HNFP; (2) to estimate the carbon sinks and sink potentials of a forest under a long-term time series in HNFP; and (3) to investigate the influence of environmental factors on the magnitudes and paths of the carbon sink potentials of different tree species in HNFP.

2. Materials and Methods

2.1. Study Area

HNFP (118°01′–118°17′ E,30°01′–30°18′ N) is located in Huangshan City in the south of Anhui Province (Figure 1); the official establishment of HNFP was approved by the former National Ministry of Forestry in 1988. From 1988 to the present, the operation of HNFP has been devoted to the protection and maintenance of its subtropical forest ecosystem, preserving the rich forest resources, wide diversity of tree species, the region's natural ecological conditions, and the integrity of the forest ecosystem. For 35 years, HNFP has been an important natural ecological reserve, forest park, geopark, and tourism area, representing one of China's most important biodiversity conservation and water conservation ecological function areas. Moreover, HNFP is located in one of the thirty-five priority areas for biodiversity conservation in China (Huangshan–Huayu Mountain Biodiversity Conservation Priority Area), and it is one of the twenty-six World Nature Conservation Units of the International Union for the Conservation of Nature (IUCN); the diversity of plants in the park is of national and global significance for conservation [43,44].

This forest park is located in the subtropical monsoon climate zone: the climate varies with altitude; the temperature decreases vertically; the north and south slopes are subject to dramatic differences in solar radiation; the local topography plays a dominant role in the formation of a special mountain monsoon climate; there is average precipitation of 2394 mm per year; and the climate is cool (an average of 7.8 degrees Celsius). The vegetation type in the forest park is mainly broad-leaved evergreen forest, with more than 900 species of trees and shrubs of 41 families, and the forest coverage rate is 84.7%, with an area of 160.6 km^2. The topography of HNFP is rich in variety, with high, mountainous terrains; height differences of up to 1700 m; and an obvious vertical distribution of vegetation, in which 94.40% of the forest patches are higher than 500 m above sea level. In summary, HNFP exhibits diversified forest types, with its origin dominated by natural forests, a

warm and humid climate, abundant rainfall, and typical features of southern subtropical montane forests.

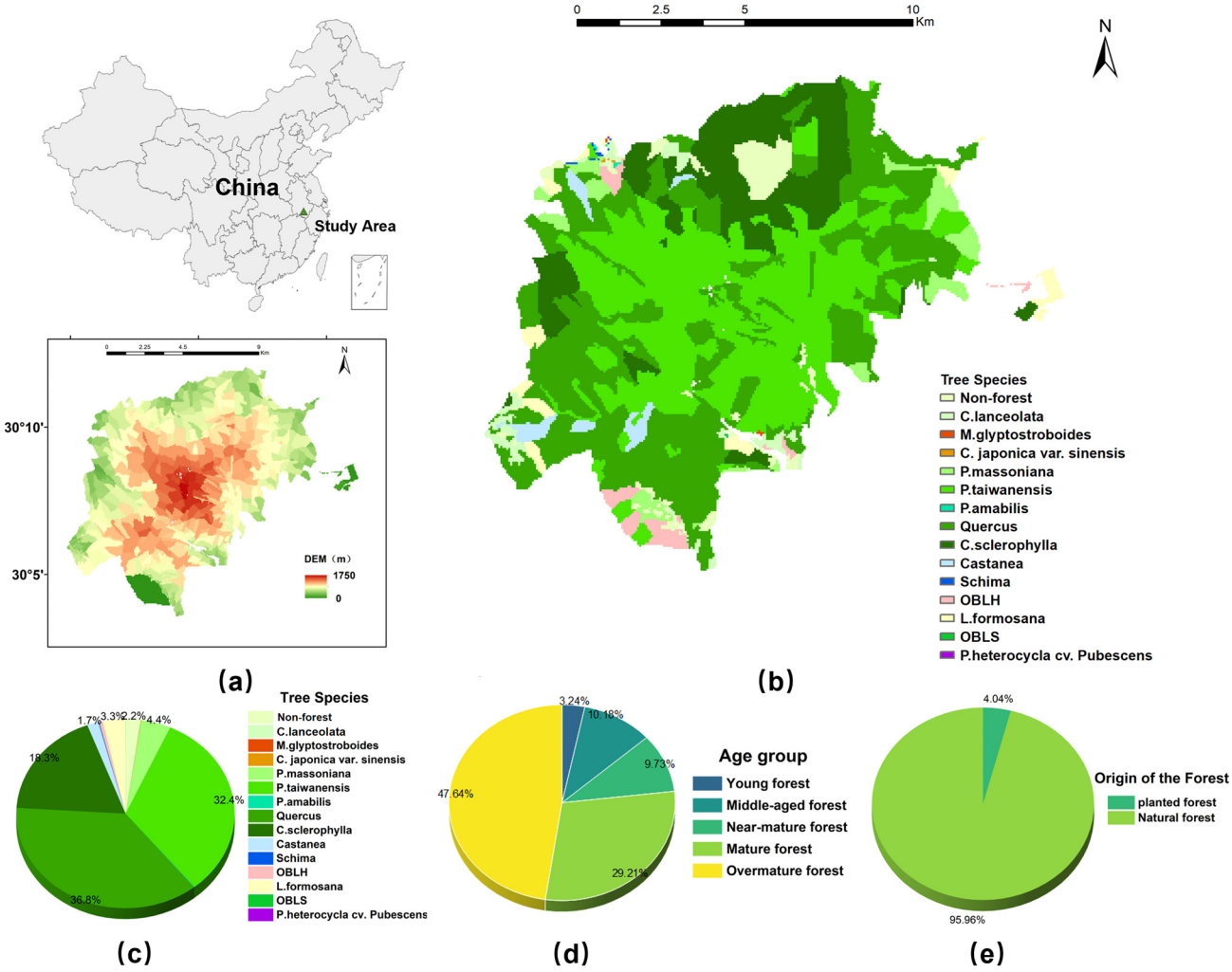

Figure 1. Geographic location, elevation, and basic information of the forest survey in HNFP. (**a**) Location and elevation. (**b**) Distribution of forest types (full species names are detailed in Section 2.2). (**c**) Area share of major dominant tree species (classes). (**d**) Age groups (young forest: ≤20; middle-aged forest: 20–30; near-mature forest: 30–40; mature forest: 40–60; and overmature forest: ≥60). (**e**) The origin of forest patches (natural/planted forests).

2.2. Data Sources

According to the "Main Technical Provisions of Forest Resources Survey", assessments of the land, trees, animals, and plants within the forest area and their environmental conditions are referred to as forest surveys. Their purpose is not only to determine the relationships between forest resources, quality, growth, and the demise of dynamic patterns in the natural environment in addition to economic and even management conditions; they are also used for the formulation and adjustment of forestry policy, the preparation of forestry plans, and the identification of forest management effect services. Such surveys also serve to formulate and adjust forestry policies, prepare forestry plans, and appraise the effectiveness of forest management, ultimately achieving the effective utilization of forest resources and improving the potential productivity of forests.

The basic data for this study were obtained from the forest management inventory data (FMID) in HNFP. There were 712 forest patches with a total area of 13,462.36 ha, which were composed of natural forest stands (naturally underplanted, artificially facilitated

regeneration, or germinated after disturbances such as natural forest logging) and planted forest stands (completely sown by machine or artificially, such as nursery, seeding, and fly sowing), of which natural forests dominated the study (95.96%). After eliminating invalid data, 658 valid forest survey patches were obtained, with a total area of 12,773.73 ha. The survey accuracy of the sampled volume and forest patch factors was ensured through systematic sampling, and the overall regional volume accuracy reached 80–85%. According to the dominant tree species in the forest sub-groups in the second land survey data, there were fourteen main species (classes) of trees, which were as follows: *Cunninghamia lanceolata (Lamb.) Hook.*, *Metasequoia glyptostroboides Hu et W. C. Cheng*, *Cryptomeria japonica var. sinensis Miq.*, *Pinus massoniana Lamb.*, *Pinus taiwanensis Hayata*, *Pseudolarix amabilis (J. Nelson) Rehder*, *Quercus*, *Castanopsis sclerophylla (Lindl. et Paxton) Schottky*, *Liquidambar formosana Hance*, *Castanea*, *Schima*, other broadleaf hardwood (OBLHother broadleaf softwood (OBLS), and *Phyllostachys heterocycle (Carr.) Mitford cv. Pubescens.* Among them, *Quercus*, *P. taiwanensis*, and *C. sclerophylla* accounted for a higher proportion of the total forest area, covering 36.8%, 32.4%, and 18.3%, respectively.

In terms of age, mature and overmature forests dominated in HNFP, with mature forests accounting for 29.20% and overmature forests accounting for 47.64% of the total forest area; 55.76% of the total forest area was over 60 years old. In total, 73 forest factors were recorded in the second survey data of HNFP, including (i) site conditions (elevation, slope direction, slope, soil thickness, humus thickness, etc.), (ii) stand characteristics (age group, average age, average diameter at breast height, average height of tree, degree of closure, etc.), and (iii) evaluation factors (public welfare forest protection class, stand protection class, etc.). These factors provided sufficient conditions for the establishment of a structural equation model. In the 658 effective forest survey patches, there were fourteen main species (classes) of trees. Due to the need to fit the growth equations, seven tree species (accounting for 98.2% of the total area) with a high number of forest sample plots were selected for the study, namely, *L. Formosana*, *C. sclerophylla*, *C. lanceolate*, OBLH, *P. massoniana*, *P. taiwanensis*, and *Quercus*.

2.3. Methods for Estimating the Forest Carbon Sink Potential

2.3.1. Estimation of Forest Carbon Stocks

The BEF method assumes that forest biomass is directly proportional to hectare volume, and the relationship between biomass and hectare volume for different forest types is obtained from the sample plot survey data, which is then converted to the carbon stock through the carbon content coefficients of various forest trees. The forest carbon sink potential can be converted to the difference between the year of maximum forest carbon stock and the forest carbon stock in a certain year; because tree growth has a maximum limit, the carbon stock of mature forests (or overmature forests) can be regarded as the maximum carbon stock in the region, so the total carbon sink potential of regional forests can be determined. The BEF method was used to estimate the biomass density of each forest patch, and then the carbon stock of the corresponding tree species was obtained through the carbon content coefficient. The parameter values of the BEF method were obtained through reference [45,46]. Firstly, the biomass conversion factor was calculated according to the hectares of standing trees in each patch, and then the biomass density was calculated. The equations are as follows:

$$BEF = a + \frac{b}{x} \quad (1)$$

$$B = BEF * X \quad (2)$$

where X in Equations (1) and (2) is the volume density (m^3/ha) of a patch (data from the FMID), B is the biomass density, a and b are constants for the forest type, and BEF is the biomass conversion factor. The biomass density calculated by this method is the average biomass density of the forest type at that age.

2.3.2. Estimation of the Forest Carbon Sink Potential

In this study, a space-for-time substitution approach was employed, leveraging data from the second national forest inventory to model the relationship between biomass density and forest age. This yielded estimates of biomass density growth for various species of trees in the Huangshan region over an extended temporal sequence from 2014 to 2060.

Two prominent growth functions, the Richard–Chapman and logistic growth models, were utilized to perform the nonlinear fitting of biomass density against forest age for a given tree species. The Richard–Chapman growth function is adaptable to a wide range of biological growth patterns, from unimodal to asymmetric S-shaped curves, by adjusting its parameters. It is particularly adept at capturing the early rapid and later slow stages of forest growth, offering greater accuracy with larger datasets. Conversely, the logistic growth function aptly describes the tendency of forest growth to stabilize after a certain point, which is crucial for simulating the carbon sink potential of forests as they mature. This function is more applicable when the dataset is of moderate size. Fitting results were tested using the highest coefficient of determination (R^2) and the *p*-value, and the results were cross-validated through the leave-one-out cross validation to ensure the accuracy of the model. The equations are as follows:

$$\text{Richard} - \text{Chapman} : y = a\left(1 - e^{-bt}\right)^c \tag{3}$$

$$\text{Logistic} : y = \frac{w}{1 + ke^{-at}} \tag{4}$$

where y is the biomass density of a patch, t is the stand age of trees, a, b, c, w, and k are the fitting parameters of the corresponding functions (a in the Richard–Chapman function and w in the logistic equation represent the maximum biomass density of a tree species under the natural growing conditions), and the maximum biomass density of overmature forests of the corresponding species in the HNFP area was taken as the value. The Chapman equation and Slogistic3 equation were used in Origin2021 for model fitting.

Assuming that there will be no deforestation or death of forests in HNFP before 2060, the carbon stock of the existing forests in a certain year in the future can be calculated using the corresponding growth function, taking the logistic growth equation as an example; the equation is as follows:

$$C_T = V * \gamma * \frac{w}{1 + ke^{-at}} \tag{5}$$

where C_T denotes the carbon stock of a patch in year T, V is the patch area, γ is the carbon content coefficient of the main tree species of the corresponding patch, w, k, and a are the fitting parameters of the logistic equation for the species, and t is the stand age of the tree species of the patch in a corresponding year.

Carbon sink capacity is the ability of vegetation to fix carbon per unit of time, expressed as the increase in carbon stocks over time. When the forest carbon density is relatively stable, the carbon sink potential is the difference between the carbon stock that tends to reach its maximum value and the current year's carbon stock. The carbon sink potential is calculated through the following equation:

$$CS = C_T - C_{T-1} \tag{6}$$

where the annual carbon sink, CS, of a given patch is the difference between the carbon stock, C_T, of the neighboring year and the corresponding carbon stock, C_{T-1}, and the current carbon sink potential is the difference between the year of the largest carbon stock and the current year's carbon stock.

2.3.3. Influencing Factor Analysis Method

Multiple correlation diagnostics were performed first to calculate the variance inflation factor (VIF), as shown in Equation (7):

$$\mathrm{VIF} = \frac{1}{1 - \mathrm{R}^2} \tag{7}$$

where R^2 is the coefficient of determination of the regression of a factor on other independent variables when it is the dependent variable. Generally, a VIF greater than 10 is considered indicative of strong multicollinearity [47], which may affect the stability of model parameter estimation. By eliminating variables with high VIF values, we ensured that the independent variables in the model remained relatively autonomous, reducing bias in parameter estimation and providing a solid foundation for subsequent SEM.

Structural equation modelling is a method for constructing, estimating, and testing causal relationship models. The model may include observable manifest variables as well as latent variables that cannot be directly observed. SEM can replace multiple regression, path analysis, factor analysis, and analysis of covariance, among other methods, to clearly analyze the impact of individual indicators on the overall system and the inter-relationships between them. Piecewise structural equation modelling (pSEM) extends traditional SEM to handle non-normal distributions and hierarchical structures, which we employed to further investigate the relationships between geographical factors and the carbon sink potential. We utilized the following five indices [39,48,49]: degrees of freedom (DF), *p*-value, standardized root mean square residual (SRMR), root mean square error of approximation (RMSEA), and the goodness-of-fit index (GFI). DF reflects complexity, with lower values typically indicating a more parsimonious model. The *p*-value is used to test the overall statistical significance of a model, with a significant *p*-value (<0.05) suggesting a good fit to the data. The SRMR is a measure of the discrepancy between observed and model-predicted values, with lower SRMR values (<0.08) indicating smaller residuals and a better fit. The RMSEA takes into account model complexity, with smaller values indicating a higher degree of fit between the model and observed data; RMSEA values less than 0.06 are generally considered indicative of an excellent model fit. The GFI measures the fit of the model relative to a perfect model, with values close to 1 indicating a very good fit. These analyses were implemented using the piecewiseSEM and lavaan packages in R 4.2.3.

3. Results

3.1. Growth Function Selection and Forest Carbon Stock Distribution

We explored the major tree species in the HNFP through Richard–Chapman and Logistic growth functions. The results of the fitting are shown in Figure 2 and Table 1. The results showed that the overall fitting of the two growth functions for the seven major tree species were better in HNFP, in which the growth functions of six tree species were successfully fitted using the Richard–Chapman growth function, with an R^2 value greater than 0.85, and the growth functions of seven tree species were successfully fitted using the logistic growth function, with an R^2 value greater than 0.90. All of the fitting results of the logistic growth function for all tree species were better than those obtained with the Richard–Chapman growth function. This indicates that the logistic growth function is more in line with the growth pattern of trees in the study area, and that it has better applicability to the estimation of forest biomass in HNFP; therefore, the results of the logistic growth function were used for the calculation of carbon stocks and the carbon sinks of all tree species. The logistic growth function describes the relationship between forest biomass and the forest age of the dominant species, which provides a basis for more accurate estimations of the carbon stock and sink potential.

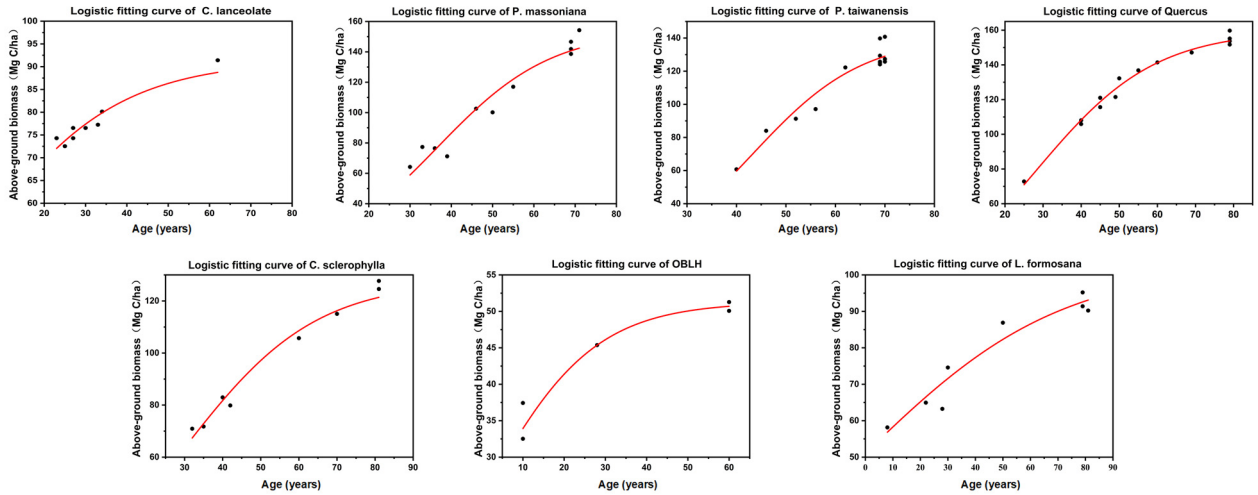

Figure 2. Fitting of growth functions for key tree species.

Table 1. BEF parameters and growth function fitting parameters.

Tree Species	Biomass Expansion Factor		Richard-Chapman Fitting Curve				Logistic Fitting Curve				
	BEF = a + b/V		$y=a(1-e^{-bx})^c$				$y=\frac{w}{1+ke^{-at}}$				
	a	b	a	b	c	R^2	w	a	k	R^2	*p*
L. formosana	0.475	30.603					102.816	0.028 ± 0.011	1.012 ± 0.159	0.944	<0.01
C. sclerophylla	1.036	8.059	127.682	0.054	3.225	0.953	127.682	0.058 ± 0.006	5.75 ± 1.401	0.975	<0.01
C. lanceolate	0.400	22.541	91.404	0.046	0.573	0.898	91.404	0.056 ± 0.012	0.979 ± 0.340	0.915	<0.01
OBLH	0.644	8.310	51.274	0.054	0.472	0.937	51.274	0.076 ± 0.015	1.094 ± 0.190	0.938	<0.01
P. massoniana	0.801	4.055	154.243	0.057	5.045	0.929	154.243	0.072 ± 0.065	14.224 ± 4.136	0.948	<0.01
P. taiwanensis	0.517	33.238	140.732	0.075	17.504	0.925	140.732	0.090 ± 0.006	50.005 ± 18.162	0.934	<0.01
Quercus	1.145	8.547	159.727	0.054	2.558	0.973	159.727	0.064 ± 0.003	6.266 ± 0.850	0.986	<0.01

For the Biomass expansion factor, a and b are constants for different forest types; for the Richard–Chapman fitting curve, a is the maximum biomass, and b and c are coefficients determining the growth rate; for the logistic fitting curve, w is the maximum growth, and a and k are coefficients determining the growth rate.

In 2014, the average carbon density of HNFP was 75.08 t/ha, the pattern of carbon density was higher in the central and northeastern regions and lower in the northern and southern regions, and most of the areas with high carbon density were distributed in blocks, while the areas with low carbon density were distributed sporadically. At the same time, to better understand the distribution characteristics of carbon stocks of each tree species, we divided the altitude into low altitude (0–600 m), middle altitude (600–1200 m), and high altitude (1200–1800 m), and we analyzed the contribution of carbon densities of different age groups of different tree species at different altitudes, as shown in Figure 3. Forest patches were more frequent in the middle-elevation interval, and the average carbon density of tree species at this elevation was 69.72 t/ha, although there was a considerable difference between the carbon densities of young forests and overmature forests, which were 20.18 t/ha and 83.23 t/ha, respectively. The tree species *Quercus* and *P. taiwanensis* contributed the most to the average carbon density at this elevation, accounting for 52.84% and 20.75%, respectively. In the low-elevation zone, the average carbon density of tree species was 55.55 t/ ha, to which *Quercus* contributed the most, accounting for 27.35%, and the carbon density of other tree species accounted for a relatively similar proportion. In the high-elevation area, the tree age group type was dominated by mature forests and overmature forests, and the average carbon density of tree species at this elevation was the highest at 83.54 t/ha, which was mostly represented by the tree species *P. taiwanensis* and *Quercus*, accounting for 72.95% and 24.34%, respectively. In the study area, the carbon density increased with elevation in the low-, middle-, and high-elevation zones, and the

carbon density of overmature or mature forests was the highest in one elevation zone, which was in line with the law of tree growth.

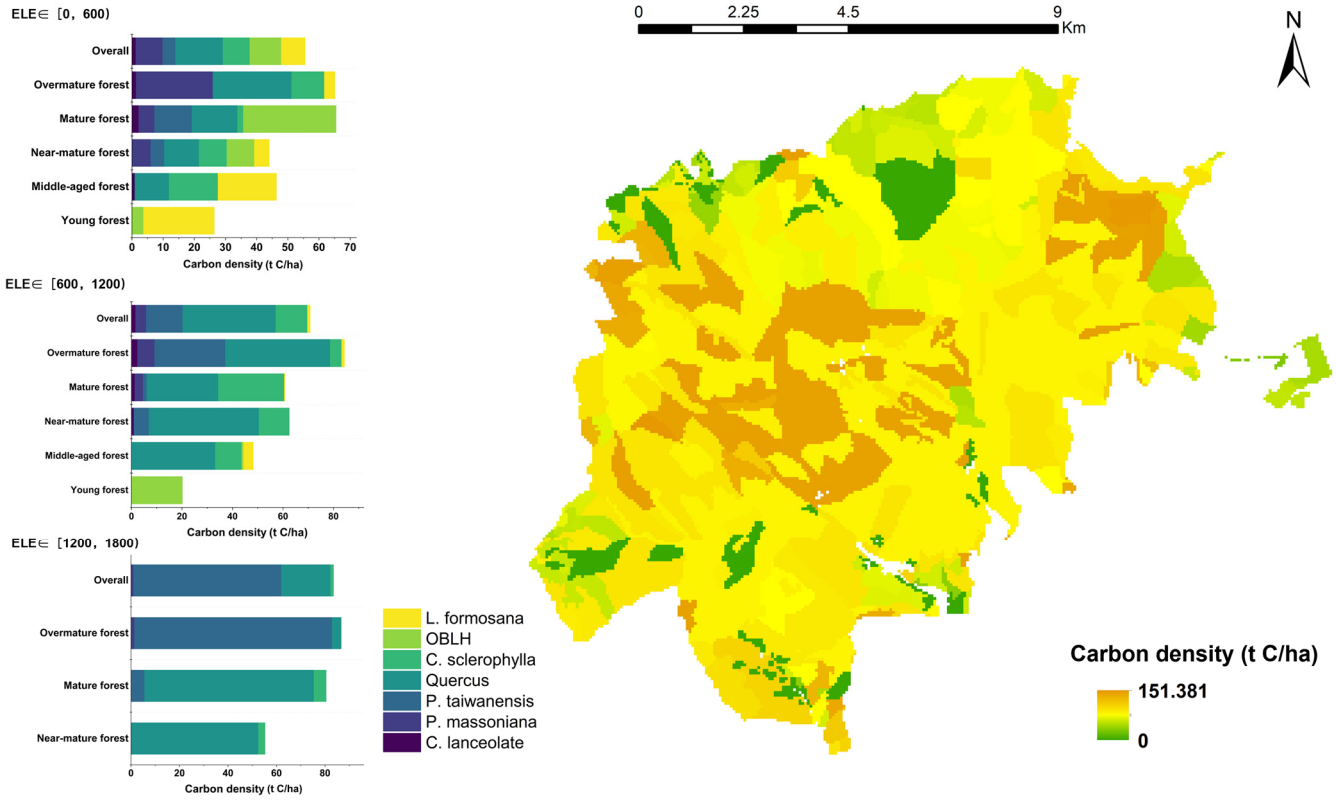

Figure 3. Characteristics of the current carbon sink capacity of forests in HNFP. The geographical distribution map shows the spatial distribution of forest carbon density in 2014; the carbon density stacking graphs show the percentage of carbon density of each age class forest type in HNFP at elevation gradients of (0 to 600), (600 to 1200), and (1200 to 1800).

In 2014, the total forest stock of HNFP was 1.38 $\times$ 10^6 m^3, the biomass was approximately 1.92 $\times$ 10^6 t, and the total forest carbon stock was approximately 9.59 $\times$ 10^5 t. Carbon stock responded to the overall status of different tree species. Among them, *Quercus* and *P. taiwanensis* contributed the most to the carbon stock of HNFP, with 3.98 $\times$ 10^5 t and 3.45 $\times$ 10^5 t, respectively, accounting for 41.50%, and 35.97% of the total forest carbon stock of HNFP in 2014, whereas *L. Formosana*, OBLH, and *C. lanceolate* contributed less to the carbon stock of HNFP, accounting for a total of 4.93% of the forest carbon stock of HNFP.

3.2. Analysis of Spatial and Temporal Patterns of Forest Carbon Sinks

According to the forest age distribution of existing forests in HNFP, the relationships between the biomass of the tree species and the forest age were explored with the growth function, which was used to obtain the relationship between the carbon stock of the tree species and the forest age and to obtain the spatial and temporal pattern of carbon sinks in HNFP from 2014 to 2060. From Figure 4, it can be seen that the carbon stock will continue to grow until 2060, although the carbon stock growth rate will slow down by 2060. *Quercus* and *P. taiwanensis* will consistently contribute the most to the carbon stock, and the share of the carbon stock of each tree species presents a relatively stable state. From 2014 to 2060, the carbon stock of HNFP will keep rising, and in 2060, it is expected that the total forest carbon stock of HNFP will reach 11.17 $\times$ 10^5 t, which is an increase of 1.58 $\times$ 10^5 t compared with that in 2014. Remaining the most important contributors to the carbon

stock of HNFP, *Quercus* and *P. taiwanensis* will account for 76% of the total forest carbon stock in 2060.

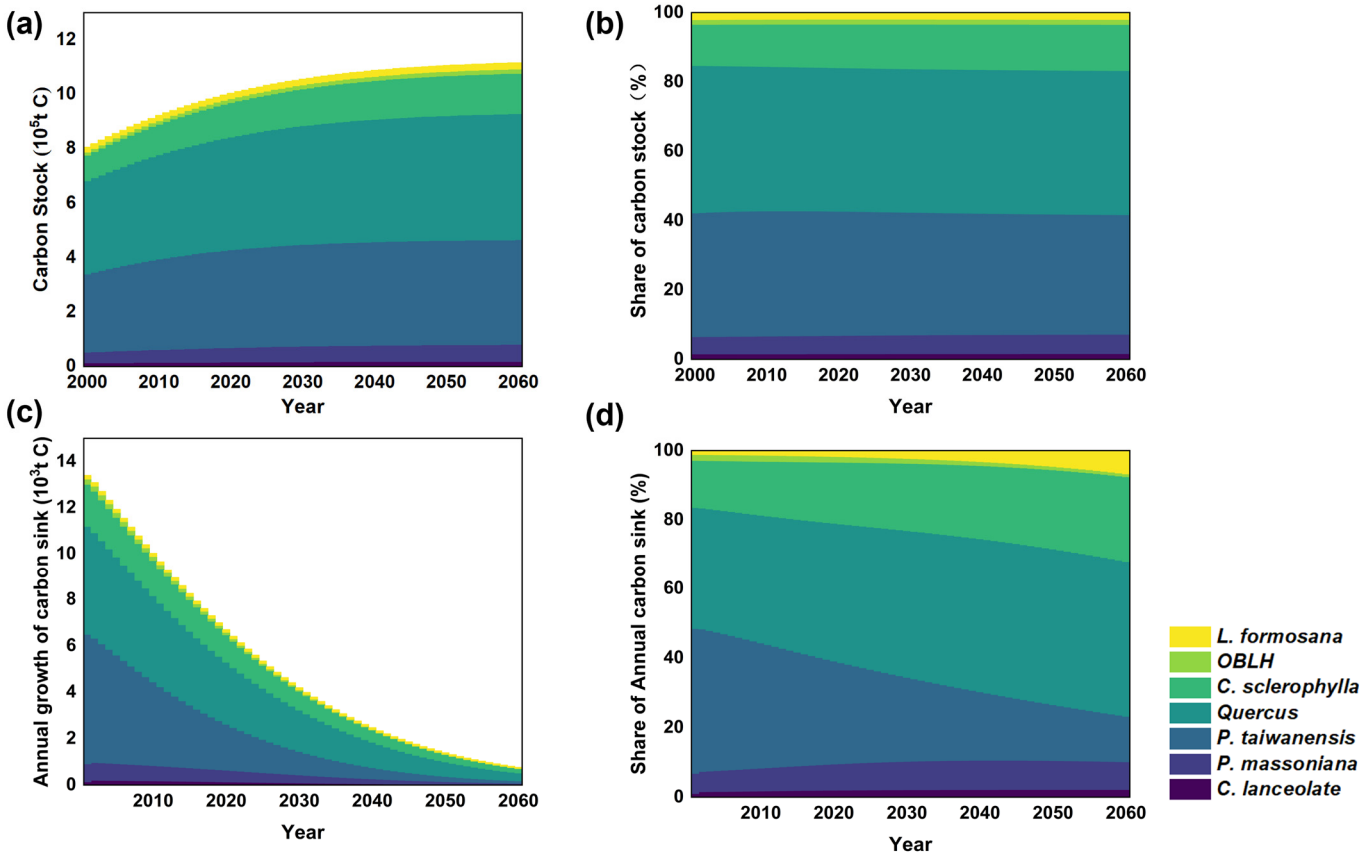

Figure 4. Carbon sink potential of different tree species from 2000 to 2060: (**a**) changes in carbon stocks of different tree species; (**b**) contributions of different tree species to the total forest carbon stocks; (**c**) changes in annual carbon sinks of tree species; and (**d**) contributions of different tree species types to the total annual carbon sinks.

Based on the carbon stock changes in the forests of HNFP under the time series of 2014–2060, the annual carbon sink, as well as the carbon sink potential of HNFP, can be obtained. The total carbon sink potential of forest trees in HNFP in 2014–2060 is 3.15×10^5 t, of which *Quercus* and *P. taiwanensis* exhibit the largest carbon sink potentials, of 1.32×10^5 t and 0.79×10^5 t, respectively. It can be seen from Table 2 and Figure 4c,d that in the years 2014–2060, the carbon sinks of each tree species, as well as the total forest carbon sink in HNFP, exhibit downward trends. From Figure 1, it can be seen that the age structure of Huangshan's forests has developed past being youthful, due to the age group of each tree species in the Huangshan Mountains being dominated by mature forests and overmature forests, generating a phenomenon of increased carbon sink capacity. Regarding *Quercus* and *P. taiwanensis*, which contribute the most to the carbon sinks in the Huangshan Mountains, the annual carbon sink contribution ratio of *Quercus* will still increase due to its large forest area, while the annual carbon sink contribution ratio of *P. taiwanensis* will decrease due to its large forest age structure, even though it accounts for a large area. It is worth mentioning that *C. sclerophylla* has the highest annual average hectare carbon sink capacity during the period of 2014–2060 due to its younger age distribution.

Table 2. Status of the carbon density/carbon stock of different tree species.

Tree Species	Forest Volume (ha)	Forest Volume Density (m^3/ha)	Tree Biomass ($\times 10^5$t)	Forest Carbon Stock ($\times 10^5$t)	Forest Carbon Density (t/ha)	Total Carbon Sink ($\times 10^3$t)	Forest Carbon Sink Intensity Growth (t/ha/a)
L. formosana	404.23	74.52	0.38	0.19	46.05	3.90	0.21
C. sclerophylla	2214.71	79.18	2.36	1.18	53.42	30.28	0.30
C. lanceolate	269.67	147.13	0.30	0.15	55.62	3.25	0.26
OBLH	207.46	53.45	0.28	0.14	66.01	2.26	0.24
P. massoniana	608.09	137.56	1.00	0.50	81.98	12.40	0.44
P. taiwanensis	4276.29	135.28	6.90	3.45	80.78	39.69	0.20
Quercus	4793.28	98.13	7.96	3.98	83.01	65.77	0.30
overall	12,773.73	103.61	19.18	9.59	75.06	157.55	0.27

3.3. Analysis of the Forest Carbon Sink Potential

From the spatial and temporal distribution of carbon sinks in HNFP, the total carbon sink of Huangshan forests from 2014 to 2015 was 8.26 $\times$ 10^3 t. Among them, *Quercus*, *P. taiwanensis*, and *C. sclerophylla* contributed the most to the carbon sink in HNFP, with values of 3.18 $\times$ 10^3 t, 2.70 $\times$ 10^3 t, and 1.37 $\times 10^3$ t, accounting for 38%, 33%, and 16% of the total forest carbon sink of HNFP in 2014. Before 2060, the carbon sink potentials of *L. Formosana*, *C. sclerophylla*, *C. lanceolate* OBLH, *P. massoniana*, *P. taiwanensis*, and *Quercus* were 1.18 $\times$ 10^4 t, 1.06 $\times$ 10^5 t, 1.52 $\times$ 10^4 t, 9.87 $\times$ 10^3 t, 4.15 $\times$ 10^4 t, 1.96 $\times$ 10^5 t, and 2.43 $\times$ 10^5 t, respectively, among which *Quercus* and *P. taiwanensis* had the highest potentials for total forest carbon sink due to their large forest areas. The tree species with the highest average carbon sink potential per hectare was *P. massoniana*, with an average carbon sink potential of up to 68.26 t/ha.

According to Figure 5, the highest carbon sink potential of HNFP is 87.56 t/ha; the distribution of the carbon sink potential was high at the edge and low in the middle. In comparison with Figure 1, it can be observed that the areas with high carbon sink potential were mainly the younger patches of *P. massoniana* and *P. taiwanensis*, due to the high bulk densities of both these tree species; in addition, the patches with high carbon sink potential were preferentially concentrated in low-altitude areas.

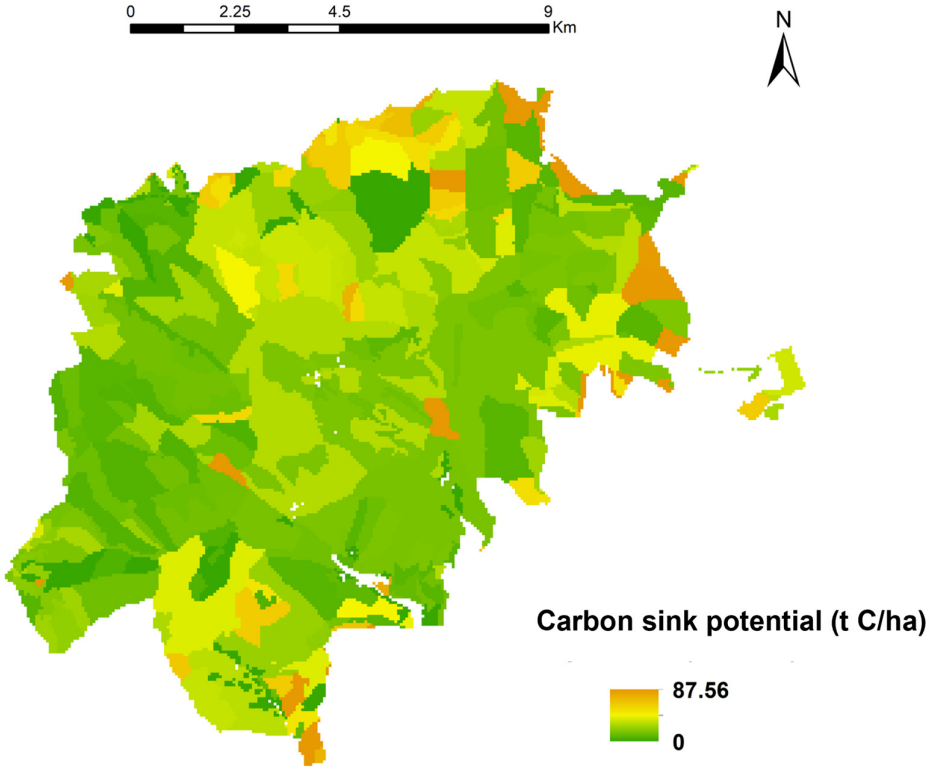

Figure 5. Distribution of the forest carbon sink potential in HNFP.

3.4. Exploration of Factors Influencing the Carbon Sink Potential

First, we screened and diagnosed the multiple correlations of several influencing factors, excluded the influencing factors with multiple covariance, and finally selected the slope, slope position, slope direction, elevation, soil thickness, humus thickness, depression, elevation, and tree age as the influencing factors to be used to construct the structural equation model with the carbon sink potential of the seven major tree species in HNFP.

For *P. taiwanensis* (Figure 6), it was found that the carbon sink potential was mainly affected by the slope position (standardized total effect value (STEV) = 0.122 *), tree age (STEV = −0.733 ***), soil thickness (STEV = −0.145 *), and elevation (STEV = 0.142 *), with tree age having the greatest effect on the carbon sink potential. Among the geographic factors, elevation had the greatest effect on the carbon sink of *P. taiwanensis*, and elevation indirectly affected the carbon sink potential of *P. taiwanensis* by influencing the slope, soil thickness, and tree age factors [12]. The soil thickness and slope indirectly affected the carbon sink potential of *P. taiwanensis* by influencing the age of the trees, while slope also affected the carbon sink potential of *P. taiwanensis* by influencing the thickness of the soil layer and the direction of the slope.

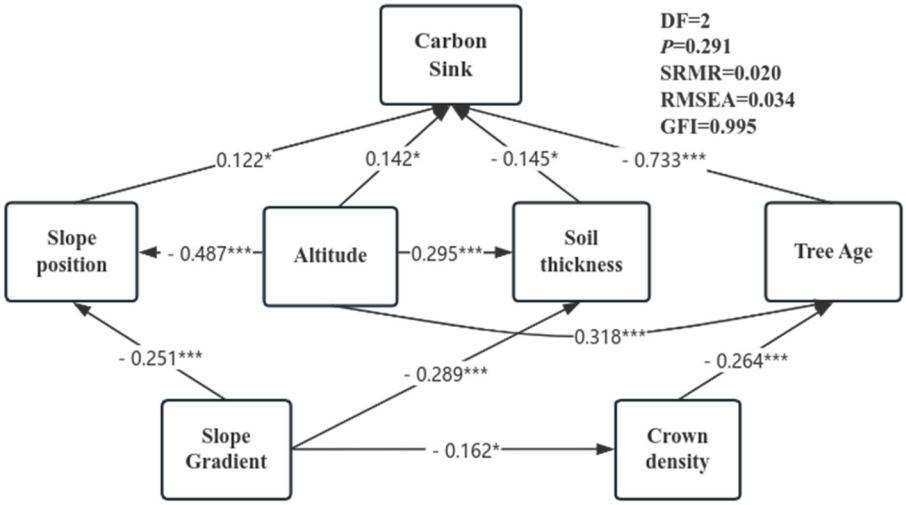

Figure 6. SEM of carbon sink-influencing factors of *P. taiwanensis*. ("*" indicates a significance level of 0.05, suggesting a 95% confidence in the observed relationships or differences. "***" signifies an even higher level of statistical significance at 0.001, offering a 99.9% confidence level).

For *Quercus* (Figure 7), its carbon sink potential was mainly affected by the direct influences of the degree of depression (STEV = −0.259 ***), tree age (STEV = −0.637 ***), and soil thickness (STEV = 0.161 **), among which age had the greatest influence on the potential of carbon sinks, followed by the degree of depression. Among the geographic factors, slope had the greatest effect on *Quercus* carbon sinks, and it indirectly affected the carbon sink potential of *P. taiwanensis* by influencing soil thickness and tree age. Elevation affected the carbon sink potential by indirectly influencing the soil thickness and slope direction, which correlates with the age of the trees; slope position also affected the carbon sink potential by influencing the age of the trees.

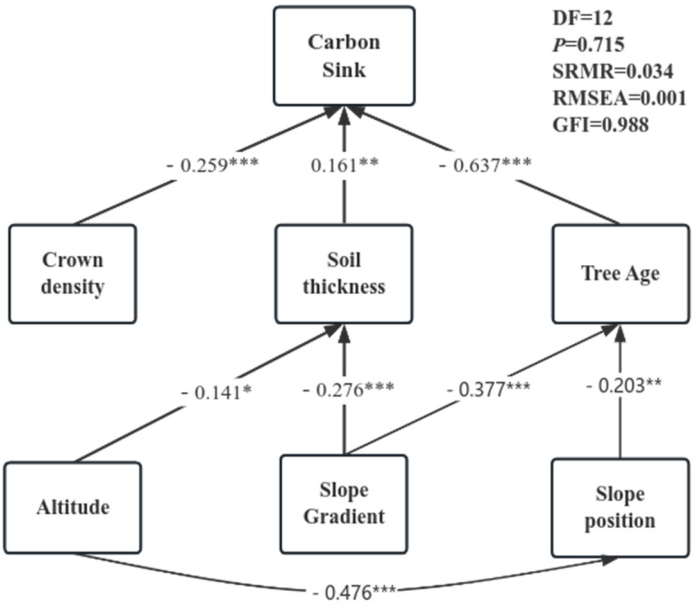

Figure 7. SEM of carbon sink influencing factors of *Quercus*. ("*" indicates a significance level of 0.05, suggesting a 95% confidence in the observed relationships or differences. "**" represents a more stringent significance level of 0.01, providing a 99% confidence level. "***" signifies an even higher level of statistical significance at 0.001, offering a 99.9% confidence level).

For *C. sclerophylla* (Figure 8), its carbon sink potential was mainly affected by the direct effects of depression (STEV = −0.270 *), tree age (STEV = −0.462 ***), and soil thickness (STEV = −0.274 *), with tree age having the greatest effect on the carbon sink potential, followed by soil thickness. Among the geographic factors, elevation indirectly affected the carbon sink potential of *C. sclerophylla* by influencing soil thickness and depression. Slope position indirectly affected the carbon sink potential by influencing the closure and tree age, and the slope also affected the carbon sink potential by influencing the soil thickness.

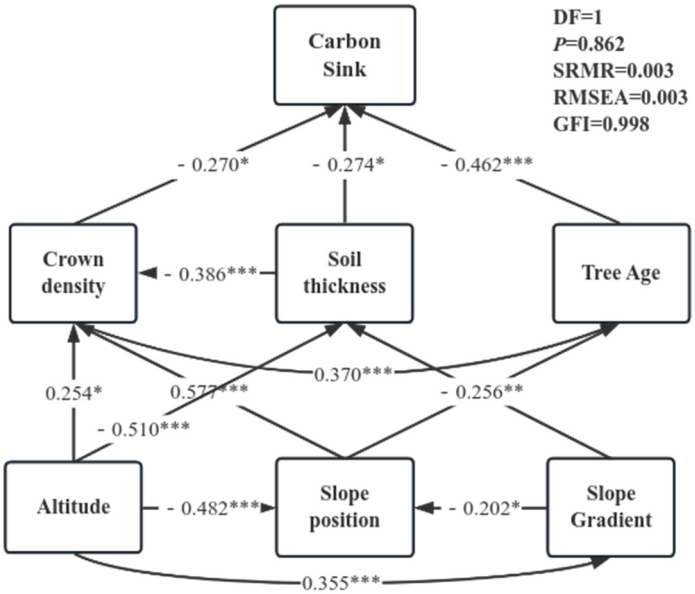

Figure 8. SEM of factors influencing the carbon sink of *C. sclerophylla*. ("*" indicates a significance level of 0.05, suggesting a 95% confidence in the observed relationships or differences. "**" represents a more stringent significance level of 0.01, providing a 99% confidence level. "***" signifies an even higher level of statistical significance at 0.001, offering a 99.9% confidence level).

4. Discussion

4.1. Assessment of Forest Carbon Stock and Sink Potential

The method of constructing biomass–age relationships based on species growth functions is now one of the main techniques for estimating forest biomass carbon stocks and predicting future forest carbon sink potentials. Several studies have used the biomass–age method to estimate the carbon sink potential of regional forests at large regional scales, such as nationally and provincially, as well as at smaller regional scales. When using this method in small areas, it is necessary to obtain a biomass–age growth function that is as accurate as possible to improve the accuracy and precision of assessments of regional carbon stock and sink potential.

In this study, taking into account the differences between tree species, the growth trends may be different during the growth processes; therefore, two growth functions were used to fit the biomass–age function of each tree species to select the growth function that is more suitable for the growth process. At the same time, the maximum biomass of tree species in different regions are also different due to variable geographic and climatic factors in the region. When setting the maximum biomass of tree species in the function, the maximum biomass of overmature forest of the species in the study area was taken as the appropriate value to derive a biomass–story–age function that was more in line with the study area. The biomass–age function of the dominant tree species in the Huangshan Mountain region obtained in this study was more representative of the growth characteristics of the tree species and the geographic and climatic environment of the region, which was more accurate under the limited data on forest biomass and forest age.

In this study, we obtained an average carbon density of 75.08 t/ha and an average sink potential of 11.70 t/ha in HNFP in 2014. In contrast to some studies on carbon stock and sink potential in Anhui Province, Ji et al. [50] used the BIOME4 model to estimate that the forest carbon density in Anhui Province in 2009 could reach up to 150.4 t/ha for young forests and 464.9 t/ha for overstory forests; Li et al. [15]. used the biomass-accumulation function to estimate the forest carbon density in Anhui Province in 2014 to be between 12.02 and 20.70 t/ha, with a sink potential of 35.67 t/ha. The results of this study show that the forest carbon density in the Huangshan region is between the two, and as a national forest park is higher than the national average forest vegetation carbon density level of 41–43 t/ha [51], this is more reasonable. Figure 4 indicates that the carbon stock of HNFP will rise less from 2014 to 2060, and the carbon stock in 2060 will only be 16% higher than the carbon stock in 2014. From Figure 1, an analysis of the structure of forest types in the study area, it can be found that *Quercus*, *P. taiwanensis*, and *C. sclerophylla* occupy 36.8%, 32.4%, and 18.3% of the forest area in HNFP, respectively, which altogether accounts for 87.5% of the total HNFP forest area. Moreover, Figure 1 shows the age structure of *Quercus*, *C. sclerophylla*, and *P. taiwanensis*, with the highest area covered by aging forest, and the base carbon stock already very high. Here, 91.6% of the total sample plots of *P. taiwanensis* were overmature forests. Due to the age structures of *Quercus*, *P. taiwanensis*, and *C. sclerophylla* being large, with the small age structures of *L. Formosana* and OBLH, the growth of carbon stock is limited; thus, the growth of carbon stock in HNFP will be small in the period from 2014 to 2060. Meanwhile, the average carbon sink potential of the forests in HNFP is relatively low compared with the results of some other studies, which is due to the large age structure of the forests and the high base carbon stock. The forests in the study area have made a large contribution to carbon sinks at this stage, but the carbon sink potential is not high because of the large age structure of the forests, and it will be necessary to adjust this age structure through future management practices to achieve greater carbon sink potential in the forests in the study area.

4.2. Factors Influencing the Forest Carbon Sink Potential

Based on the age–biomass growth of different tree species in the study area, the carbon stock and future carbon sink potential of HNFP were estimated. The carbon density changes greatly with aging from young to mature forests; then, growing from mature

to overmature forests, the carbon density still increases, but more slowly. This growth trend of forest carbon stock is consistent with the results of some previous studies [41]. In the Huangshan region, due to the large age structure of the forest, the three main tree species occupying the largest area are dominated by mature forests and overmature forests. Although mature forests and overmature forests will continue to accumulate carbon with the increase in forest age, the carbon stock of the whole region will grow slowly in the future. However, the high carbon density of HNFP at this stage indicates that the area has already brought huge carbon sinks and ecological value, which are closely related to the long-term aims of ecological protection and continuous afforestation in the area. In the next forty years, China will continue to carry out afforestation, ecological restoration, and eco-region construction projects, and to increase the forest area to achieve the goals of peak carbon emissions by 2030 and future carbon neutrality. According to the China Forestry Sustainable Development Strategy Research Group, the quantity and quality of existing Chinese forests are expected to enter a stable development phase, which means that the increase in the carbon sink potential of forests may be limited. Therefore, it is important to discuss multiple influencing factors and sink potentials for different tree species and to study under which environment different tree species will have greater sink potentials.

SEM for various tree species revealed that the factors influencing carbon sink potential differ between species. For *P. taiwanensis*, the slope position exerts a direct positive effect on the carbon sink potential, while soil thickness has a direct negative impact. Although altitude contributes directly and positively, its effects on slope position, soil thickness, and age ultimately exert a negative influence on carbon sink potential. Crown density indirectly affects the carbon sink potential through forest age, having a positive impact. Slope gradient has a weaker negative effect on carbon sink potential, which is indirectly influenced by slope position, soil thickness, and crown density.

For *Quercus*, altitude indirectly negatively affects the carbon sink potential through soil thickness and age, while the slope position indirectly has a positive effect through age. Unlike *P. taiwanensis*, crown density directly negatively impacts carbon sink potential for *Quercus*, whereas soil thickness has a direct positive effect. Slope gradient indirectly exerts a positive influence on the carbon sink potential through soil thickness and forest age.

For *C. sclerophylla*, the interacting pathways among influencing factors are more complex. Crown density and soil thickness both directly negatively impact the carbon sink potential. Slope gradient indirectly has a positive effect through its influence on soil thickness. Slope position ultimately negatively affects carbon sink potential through its effects on crown density and age. Altitude exerts a positive final impact on carbon sink potential by affecting the slope position, slope gradient, and crown density.

It is evident that geographical factors have varied impacts on the carbon sink potential of different tree species. For instance, altitude has a negative effect on the carbon sink potential of *P. taiwanensis* and *Quercus* species, but a positive effect on *C. sclerophylla*. Slope gradient has a positive influence on the carbon sink potential of *Quercus* and *C. sclerophylla*, but a negative effect on *P. taiwanensis*. The pathways of influence also differ between species; for example, the carbon sink potentials of *Quercus* and *C. sclerophylla* are directly affected by crown density, soil thickness, and forest age, whereas that of *P. taiwanensis* is directly influenced by the slope position, altitude, soil thickness, and age. Unlike previous studies focused on small areas, some research [20,52] has found that site factors such as slope gradient and aspect are positively correlated with carbon sink potential because the direction and degree of slopes can redistribute light, heat, and water resources on the surface, affecting the forest's carbon sink process. However, when refining the study of influencing factors to different tree species, environmental factors can have various impacts on the carbon sink potential due to the different growth environment preferences of species; for example, *P. taiwanensis* commonly grows in high mountain areas, whereas *C. sclerophylla* prefers lower altitudes.

Therefore, different planting sites and management strategies are required for different tree species. For example, when planting *P. taiwanensis*, a reforestation species in the

study area, it is not sufficient to merely consider the species' habit of growing at high altitudes; factors such as soil thickness and slope position must also be taken into account. Selecting site conditions that are more suitable for the specific tree species can enhance its carbon sink potential, providing greater ecological value over the long term. Ideally, detailed reforestation management tailored to the tree species can significantly increase the forest's carbon sink capacity, offering insights for the enhancement of China's future forest carbon sinks.

4.3. Uncertainties and Potential Constraints

Carbon stocks in forest ecosystems include the carbon stocks in the aboveground forest vegetation and apomictic parts and the carbon stocks in the belowground soil parts. In this study, the carbon stock in the forest ecosystem of HNFP was calculated only for the tree layer, and the carbon stock of the above categories was not calculated due to the lack of data for the shrub layer, herb layer, dead wood and humus layer, and the soil layer; therefore, the carbon stock in the forest ecosystem of HNFP was greatly underestimated. Secondly, the maximum carbon sink potential determined from the spatial and temporal carbon storage curves obtained from the biomass–age function in this study is the maximum carbon sink potential that could be realized under the ideal situation of assuming no forest disease or death. In reality, forests are subject to various kinds of disturbances, as well as deaths during the growth process, which greatly reduce the ideal carbon sink potential [53].

At the same time, estimations of carbon stock and carbon sink potential in the HNFP area were only performed for the main tree species in the area, which underestimated the carbon stock and carbon sink potential of the Huangshan area to a certain extent. HNFP is a protected area; thus, anthropogenic interference was ignored, and climate factors such as rainfall, temperature, and humidity were not included in the structural equations because of the small study area. In fact, by including anthropogenic and climatic factors in SEM, the effects and pathways of various factors on the potential of carbon sinks can be more clearly observed.

Regarding the limitations of this study, although numerous investigations [20,46] have employed FMID data to explore aspects of carbon storage, sequestration, and potential sequestration, it is possible that the precision of FMID data may not match that acquired through forest inventory methods, which involve measurements of individual trees within a region. The latter requires the investment of substantial time and high costs for a large number of professionals, which, in turn, constrains the accuracy of the outcomes derived from related research. This study, initially performed with FMID data and after calculating growth curves by tree species, has yielded relatively accurate results. Future work may include detailed regional forest surveys to obtain more precise data, which will enable more accurate construction of SEM models.

Secondly, temperature and humidity are critical factors influencing tree growth and carbon sink potential. By 2060, with the concerted efforts of nations worldwide, the environmental temperature and humidity within the study area are expected to undergo certain changes. This research did not incorporate a study of the variations in carbon storage, sequestration, and sequestration potential in response to changes in temperature and humidity before 2060, which is incongruent with the actual growth conditions of forests. Subsequent studies considering temperature and humidity factors within the tree growth models will enhance the reliability of the results. In addition, the BEF coefficient may actually change with the growth status of the trees [27]; the dynamic BEF value was not considered in this study. SEM would also be more accurate and convincing if it was based on the potential for carbon sinks with more factors taken into account.

Finally, due to the differing adaptability of specific tree species in HNFP to regional geographic and climatic characteristics, the carbon sink potential results of the study may only apply to the HNFP region and regions with similar geographic and climatic characteristics, and the results of the study may have been different under diverse geographic or climatic conditions.

5. Conclusions

In this study, the BEF method was synergistically applied with growth functions, and through the fitting of a variety of growth functions, more accurate growth functions for the principal tree species in HNFP were determined. This yielded relatively precise values for forest carbon storage and carbon sink potential. Performing SEM for the main tree species also clarified the extent to which, and the pathways of how, environmental factors have impacts on these species.

Despite the projected continuous increase in carbon storage in HNFP until the year 2060, the rate of carbon sink growth is expected to decline, potentially reflecting the future growth conditions of most existing forests across China [12]. To meet China's carbon peak and neutrality goals, as well as global carbon neutrality objectives, enhancements in forest carbon sinks are essential. Therefore, small-scale, targeted afforestation management aimed at augmenting the carbon sink potential is undoubtedly viable. For example, the principal tree species for afforestation in HNFP are *C. lanceolate* and *P. taiwanensis*. During afforestation management, it is possible to select site conditions more conducive to these species (such as altitude and slope position), which could lead to a more optimal distribution of afforestation areas and, consequently, a higher future carbon sink capability.

It is foreseeable that, in the context of the global trend towards energy conservation and emissions reductions, the calculation of more precise regional carbon storage and carbon sink potential will be increasingly utilized. Although the research findings are somewhat applicable in similar climatic zones, the climates of afforestation regions in China vary considerably, as do the different tree species used for afforestation in different locales.

Future research should, therefore, investigate the factors affecting the carbon sink potential of various tree species nationally, and even globally, to provide sound afforestation guidance for larger areas. Additionally, with a substantial research data foundation, it is important to consider temporal variations in temperature and humidity, as well as changes in the BEF during trees' growth processes, and to incorporate a broader range of influencing factors into the research field. And, the intrinsic mechanisms of the complex interactions of the factors need to be revealed. This will enhance the accuracy of the results, thereby better contributing to the achievement of global carbon neutrality goals.

Author Contributions: Conceptualization, W.H. and D.Z.; methodology, W.H. and D.Z.; software, W.H. and D.Z.; validation, W.H., D.Z. and X.W.; formal analysis, W.H.; investigation, W.H.; resources, W.H.; data curation, W.H.; writing—original draft preparation, W.H.; writing—review and editing, W.H.; visualization, W.H. and D.Z.; supervision, X.W.; project administration, X.W.; funding acquisition, X.W. All authors have read and agreed to the published version of the manuscript.

Funding: This study was funded by the National Social Science Foundation Fund for Major Projects (14ZDB140) of China and the National Key Research and Development Program of China (2016YFC0502705).

Institutional Review Board Statement: Not applicable.

Informed Consent Statement: Not applicable.

Data Availability Statement: The data presented in this study are available on request from the corresponding author.

Acknowledgments: The authors are very grateful to the Data Center for Resources and Environmental Sciences, Chinese Academy of Sciences (http://www.resdc.cn (accessed on 10 April 2023)), Science and Technology Resource Service System of National Ecosystem Observation and Research Network (http://www.cnern.org.cn (accessed on 16 August 2023)).

Conflicts of Interest: The authors declare no conflicts of interest.

References

1. Neagu, O.; Teodoru, M.C. The Relationship between Economic Complexity, Energy Consumption Structure and Greenhouse Gas Emission: Heterogeneous Panel Evidence from the EU Countries. *Sustainability* **2019**, *11*, 497. [CrossRef]
2. He, Y.; Li, X.; Huang, P.; Wang, J.N. Exploring the Road toward Environmental Sustainability: Natural Resources, Renewable Energy Consumption, Economic Growth, and Greenhouse Gas Emissions. *Sustainability* **2022**, *14*, 1579. [CrossRef]
3. Gattuso, J.P.; Magnan, A.K.; Bopp, L.; Cheung, W.W.L.; Duarte, C.M.; Hinkel, J.; McLeod, E.; Micheli, F.; Oschlies, A.; Williamson, P.; et al. Ocean Solutions to Address Climate Change and Its Effects on Marine Ecosystems. *Front. Mar. Sci.* **2018**, *5*, 337. [CrossRef]
4. Zeng, Z.; Piao, S.; Li, L.Z.X.; Zhou, L.; Ciais, P.; Wang, T.; Li, Y.; Lian, X.; Wood, E.F.; Friedlingstein, P.; et al. Climate mitigation from vegetation biophysical feedbacks during the past three decades. *Nat. Clim. Chang.* **2017**, *7*, 432–436. [CrossRef]
5. Pan, Y.D.; Birdsey, R.A.; Fang, J.Y.; Houghton, R.; Kauppi, P.E.; Kurz, W.A.; Phillips, O.L.; Shvidenko, A.; Lewis, S.L.; Canadell, J.G.; et al. A Large and Persistent Carbon Sink in the World's Forests. *Science* **2011**, *333*, 988–993. [CrossRef]
6. Bonan, G.B. Forests and Climate Change: Forcings, Feedbacks, and the Climate Benefits of Forests. *Science* **2008**, *320*, 1444–1449. [CrossRef]
7. Piao, S.L.; Yin, G.D.; Tan, J.G.; Cheng, L.; Huang, M.T.; Li, Y.; Liu, R.G.; Mao, J.F.; Myneni, R.B.; Peng, S.S.; et al. Detection and attribution of vegetation greening trend in China over the last 30 years. *Glob. Chang. Biol.* **2015**, *21*, 1601–1609. [CrossRef]
8. Lu, F.; Hu, H.F.; Sun, W.J.; Zhu, J.J.; Liu, G.B.; Zhou, W.M.; Zhang, Q.F.; Shi, P.L.; Liu, X.P.; Wu, X.; et al. Effects of national ecological restoration projects on carbon sequestration in China from 2001 to 2010. *Proc. Natl. Acad. Sci. USA* **2018**, *115*, 4039–4044. [CrossRef]
9. Lehtonen, A.; Mäkipää, R.; Heikkinen, J.; Sievänen, R.; Liski, J. Biomass expansion factors (BEFs) for Scots pine, Norway spruce and birch according to stand age for boreal forests. *For. Ecol. Manag.* **2004**, *188*, 211–224. [CrossRef]
10. Peng, S.S.; Piao, S.L.; Zeng, Z.Z.; Ciais, P.; Zhou, L.M.; Li, L.Z.X.; Myneni, R.B.; Yin, Y.; Zeng, H. Afforestation in China cools local land surface temperature. *Proc. Natl. Acad. Sci. USA* **2014**, *111*, 2915–2919. [CrossRef]
11. Hong, S.; Ding, J.; Kan, F.; Xu, H.; Chen, S.; Yao, Y.; Piao, S. Asymmetry of carbon sequestrations by plant and soil after forestation regulated by soil nitrogen. *Nat. Commun.* **2023**, *14*, 3196. [CrossRef]
12. Xu, H.; Yue, C.; Zhang, Y.; Liu, D.; Piao, S. Forestation at the right time with the right species can generate persistent carbon benefits in China. *Proc. Natl. Acad. Sci. USA* **2023**, *120*, e2304988120. [CrossRef]
13. Chen, S.; Lu, N.; Fu, B.; Wang, S.; Deng, L.; Wang, L. Current and future carbon stocks of natural forests in China. *For. Ecol. Manag.* **2022**, *511*, 120137. [CrossRef]
14. Zhang, D.; Geng, X.; Chen, W.; Fang, L.; Yao, R.; Wang, X.; Zhou, X. Inconsistency of Global Vegetation Dynamics Driven by Climate Change: Evidences from Spatial Regression. *Remote Sens.* **2021**, *13*, 3442. [CrossRef]
15. Li, J.; Bai, Y.-f.; Peng, Y.; Jiang, C.-q.; Wang, S.-l.; Sun, R.; Xu, R. Carbon Accounting of Chinese Fir Plantation in Huitong, Hu'nan Province. *For. Res.* **2017**, *30*, 436–443. [CrossRef]
16. Kauppi, P.E.; Ciais, P.; Högberg, P.; Nordin, A.; Lappi, J.; Lundmark, T.; Wernick, I.K. Carbon benefits from Forest Transitions promoting biomass expansions and thickening. *Glob. Chang. Biol.* **2020**, *26*, 5365–5370. [CrossRef] [PubMed]
17. Woodall, C.W.; Walters, B.F.; Coulston, J.W.; D'Amato, A.W.; Domke, G.M.; Russell, M.B.; Sowers, P.A. Monitoring Network Confirms Land Use Change is a Substantial Component of the Forest Carbon Sink in the eastern United States. *Sci. Rep.* **2015**, *5*, 17028. [CrossRef] [PubMed]
18. Tian, X.H.; Sohngen, B.; Baker, J.; Ohrel, S.; Fawcett, A.A. Will US Forests Continue to Be a Carbon Sink? *Land Econ.* **2018**, *94*, 97–113. [CrossRef]
19. Daigneault, A.; Baker, J.S.; Guo, J.G.; Lauri, P.; Favero, A.; Forsell, N.; Johnston, C.; Ohrel, S.B.; Sohngen, B. How the future of the global forest sink depends on timber demand, forest management, and carbon policies. *Glob. Environ. Chang.-Hum. Policy Dimens.* **2022**, *76*, 102582. [CrossRef] [PubMed]
20. He, G.; Zhang, Z.D.; Zhu, Q.; Wang, W.; Peng, W.T.; Cai, Y.L. Estimating Carbon Sequestration Potential of Forest and Its Influencing Factors at Fine Spatial-Scales: A Case Study of Lushan City in Southern China. *Int. J. Environ. Res. Public Health* **2022**, *19*, 9184. [CrossRef] [PubMed]
21. Fang, J.Y.; Chen, A.P.; Peng, C.H.; Zhao, S.Q.; Ci, L. Changes in forest biomass carbon storage in China between 1949 and 1998. *Science* **2001**, *292*, 2320–2322. [CrossRef] [PubMed]
22. Richardson, A.D.; Williams, M.; Hollinger, D.Y.; Moore, D.J.P.; Dail, D.B.; Davidson, E.A.; Scott, N.A.; Evans, R.S.; Hughes, H.; Lee, J.T.; et al. Estimating parameters of a forest ecosystem C model with measurements of stocks and fluxes as joint constraints. *Oecologia* **2010**, *164*, 25–40. [CrossRef] [PubMed]
23. Zhou, T.; Shi, P.J.; Jia, G.S.; Dai, Y.J.; Zhao, X.; Wei, S.G.; Du, L.; Wu, H.; Luo, Y.Q. Age-dependent forest carbon sink: Estimation via inverse modeling. *J. Geophys. Res.-Biogeosci.* **2015**, *120*, 2473–2492. [CrossRef]
24. Song, X.W.; Gao, Y.; Wen, X.F.; Guo, D.L.; Yu, G.R.; He, N.P.; Zhang, J.Z. Carbon sequestration potential and its eco-service function in the karst area, China. *J. Geogr. Sci.* **2017**, *27*, 967–980. [CrossRef]
25. Zhang, Y.; Chen, H.Y.H. Individual size inequality links forest diversity and above-ground biomass. *J. Ecol.* **2015**, *103*, 1245–1252. [CrossRef]
26. Li, Y.C.; Li, M.Y.; Li, C.; Liu, Z.Z. Forest aboveground biomass estimation using Landsat 8 and Sentinel-1A data with machine learning algorithms. *Sci. Rep.* **2020**, *10*, 9952. [CrossRef]
27. Soares, P.; Tome, M. Biomass expansion factors for Eucalyptus globulus stands in Portugal. *For. Syst.* **2012**, *21*, 141–152. [CrossRef]

28. Brown, S.; Gillespie, A.J.R.; Lugo, A.E. Biomass estimation methods for tropical forests with applications to forest inventory data. *For. Sci.* **1989**, *35*, 881–902.
29. Feng, F.; Wang, K.C. Merging High-Resolution Satellite Surface Radiation Data with Meteorological Sunshine Duration Observations over China from 1983 to 2017. *Remote Sens.* **2021**, *13*, 602. [CrossRef]
30. Forrester, D.I.; Tachauer, I.H.H.; Annighoefer, P.; Barbeito, I.; Pretzsch, H.; Ruiz-Peinado, R.; Stark, H.; Vacchiano, G.; Zlatanov, T.; Chakraborty, T.; et al. Generalized biomass and leaf area allometric equations for European tree species incorporating stand structure, tree age and climate. *For. Ecol. Manag.* **2017**, *396*, 160–175. [CrossRef]
31. Zhao-gang, L.; Feng-ri, L. The generalized Chapman-Richards function and applications to tree and stand growth. *J. For. Res.* **2003**, *14*, 19–26. [CrossRef]
32. Dhyani, S.; Singh, A.; Gujre, N.; Joshi, R.K. Quantifying tree carbon stock in historically conserved Seminary Hills urban forest of Nagpur, India. *Acta Ecol. Sin.* **2021**, *41*, 193–203. [CrossRef]
33. Xu, L.; Shi, Y.J.; Fang, H.Y.; Zhou, G.M.; Xu, X.J.; Zhou, Y.F.; Tao, J.X.; Ji, B.Y.; Xu, J.; Li, C.; et al. Vegetation carbon stocks driven by canopy density and forest age in subtropical forest ecosystems. *Sci. Total Environ.* **2018**, *631-632*, 619–626. [CrossRef]
34. Lu, S.; Zhang, D.; Wang, L.; Dong, L.; Liu, C.; Hou, D.; Chen, G.; Qiao, X.; Wang, Y.; Guo, K. Comparison of plant diversity-carbon storage relationships along altitudinal gradients in temperate forests and shrublands. *Front. Plant Sci.* **2023**, *14*, 1120050. [CrossRef] [PubMed]
35. Wang, G.; Guan, D.S.; Xiao, L.; Peart, M.R. Forest biomass-carbon variation affected by the climatic and topographic factors in Pearl River Delta, South China. *J. Environ. Manag.* **2019**, *232*, 781–788. [CrossRef]
36. Melikov, C.H.; Bukoski, J.J.; Cook-Patton, S.C.; Ban, H.Y.; Chen, J.L.; Potts, M.D. Quantifying the Effect Size of Management Actions on Aboveground Carbon Stocks in Forest Plantations. *Curr. For. Rep.* **2023**, *9*, 131–148. [CrossRef]
37. Liu, Y.; Gao, X.; Fu, C.; Yu, G.; Liu, Z. Estimation of carbon sequestration potential of forest biomass in China based on National Forest Resources Inventory. *Acta Ecol. Sin.* **2019**, *39*, 4002–4009.
38. Zhang, C.; Deng, Q.; Liu, A.; Liu, C.; Xie, G. Effects of Stand Structure and Topography on Forest Vegetation Carbon Density in Jiangxi Province. *Forests* **2021**, *12*, 1483. [CrossRef]
39. Lefcheck, J.S. piecewiseSEM: Piecewise structural equation modelling in r for ecology, evolution, and systematics. *Methods Ecol. Evol.* **2016**, *7*, 573–579. [CrossRef]
40. Byrnes, J.E.; Reed, D.C.; Cardinale, B.J.; Cavanaugh, K.C.; Holbrook, S.J.; Schmitt, R.J. Climate-driven increases in storm frequency simplify kelp forest food webs. *Glob. Chang. Biol.* **2011**, *17*, 2513–2524. [CrossRef]
41. Duffy, J.E.; Macdonald, K.S. Kin structure, ecology and the evolution of social organization in shrimp: A comparative analysis. *Proc. R. Soc. B Biol. Sci.* **2009**, *277*, 575–584. [CrossRef]
42. Fang, W. Conservation and Planning of World Geo-heritage in Mount Huangshan. *Res. Soil Water Conserv.* **2004**, *11*, 206–208.
43. Wang, D.G. Push-pull factors in mountain resorts—A Case Study of Huangshan Mountain as World Heritage. *Chin. Geogr. Sci.* **2004**, *14*, 368–376. [CrossRef]
44. Zhang, J.H.; Zhang, Y.; Zhou, J.; Liu, Z.H.; Zhang, H.L.; Tian, Q. Tourism water footprint: An empirical analysis of Mount Huangshan. *Asia Pac. J. Tour. Res.* **2017**, *22*, 1083–1098. [CrossRef]
45. Fang, J.Y.; Guo, Z.D.; Piao, S.L.; Chen, A.P. Terrestrial vegetation carbon sinks in China, 1981–2000. *Sci. China Ser. D-Earth Sci.* **2007**, *50*, 1341–1350. [CrossRef]
46. Fang, J.Y.; Oikawa, T.; Kato, T.; Mo, W.H.; Wang, Z.H. Biomass carbon accumulation by Japan's forests from 1947 to 1995. *Glob. Biogeochem. Cycles* **2005**, *19*. [CrossRef]
47. O'Brien, R.M. A caution regarding rules of thumb for variance inflation factors. *Qual. Quant.* **2007**, *41*, 673–690. [CrossRef]
48. Jia, B.; He, J.Y.; Wang, X.J. Species asynchrony stabilizes productivity over 20 years in Northeast China. *Ecol. Evol.* **2023**, *13*, e9991. [CrossRef] [PubMed]
49. Shipley, B. The AIC model selection method applied to path analytic models compared using a d-separation test. *Ecology* **2013**, *94*, 560–564. [CrossRef] [PubMed]
50. Ji, Y.; Guo, K.; Ni, J.; Xu, X.; Wang, Z.; Wang, S. Current forest carbon stocks and carbon sequestration potential in Anhui Province, China. *Chin. J. Plant Ecol.* **2016**, *40*, 395–404.
51. Guo, Z.; Hu, H.; Li, P.; Li, N.; Fang, J. Spatio-temporal changes in biomass carbon sinks in China's forests from 1977 to 2008. *Sci. China Life Sci.* **2013**, *56*, 661–671. [CrossRef] [PubMed]
52. Wu, D.; Shao, Q.; Li, J. Effects of afforestation on carbon storage in Boyang Lake Basin, China. *Chin. Geogr. Sci.* **2013**, *23*, 647–654. [CrossRef]
53. Zhao, M.; Yang, J.; Zhao, N.; Liu, Y.; Wang, Y.; Wilson, J.P.; Yue, T. Estimation of China's forest stand biomass carbon sequestration based on the continuous biomass expansion factor model and seven forest inventories from 1977 to 2013. *For. Ecol. Manag.* **2019**, *448*, 528–534. [CrossRef]